Composites Science and Technology 68 (2008) 2551–2556

Contents lists available at ScienceDirect

Composites Science and Technology

journal homepage: www.elsevier.com/locate/compscitech

Facile monomer stabilization approach to fabricate iron/vinyl ester resin nanocomposites

Zhanhu Guo [a,*,1], Hongfei Lin [b], Amar B. Karki [c], Suying Wei [a], David P. Young [c], Sung Park [d], John Willis [d], Thomas H. Hahn [a]

[a] Mechanical and Aerospace Engineering Department, University of California, Los Angeles, CA 90095, USA
[b] Intelligent Energy, Inc., 2955 Redondo Avenue, Long Beach, CA 90806, USA
[c] Department of Physics and Astronomy, Louisiana State University, Baton Rouge, Louisiana 70803, USA
[d] Advanced Materials and Process Development, NGC ISWR, One Hornet Way, M/S: 9A45 W2 El Segundo, CA 90245, USA

ARTICLE INFO

Article history:
Received 11 March 2008
Received in revised form 7 May 2008
Accepted 15 May 2008
Available online 3 June 2008

Keywords:
A. Particle-reinforced composites
A. Polymer-matrix composites (PMCs)
A. Nanocomposites
B. Magnetic properties

ABSTRACT

Fe/Vinyl ester resin nanocomposites were fabricated by the monomer particle stabilization without any additional surfactant or coupling agent. Vinyl ester monomer serves as a coupling agent with one side covalently bound onto the nanoparticle surface by a displacement reaction and the other end copolymerized with extra vinyl ester resin to form a robust unity. The addition of iron nanoparticles favors the nanocomposite fabrication with a lower initial curing temperature. Vinyl ester resin in the nanocomposites becomes thermally stable as compared to the pure vinyl ester resin. An enhanced mechanical property is observed due to the uniform particle dispersion and the introduced interfacial covalent bondage. The iron nanoparticles become magnetically harder (with a larger coercivity) after dispersion in the vinyl ester resin matrix.

1. Introduction

Magnetic nanoparticles with a size close to the single-domain are of tremendous interest in different fields of chemistry and physics due to their unique magnetic properties such as high coercivity and chemical catalytic properties inherent with their small size and high specific surface area [1]. However, industrial applications of bare vulnerable metal nanoparticles are still a challenge due to the aggregation and easy oxidation [1,2]. To achieve a stable nanoparticle usable system, metal nanoparticles are usually stabilized by a surfactant/polymer or a noble metal shell, which reduces the particle agglomeration in a colloidal suspension or protects them from oxidation in harsh environments [3–5].

Polymeric nanocomposites reinforced with nanoparticles have attracted much interest due to their cost-effective processability and tunable physical properties such as mechanical, magnetic, optical, electric and electronic properties [4,6–10]. The use of proper functional nanoparticles within a polymeric matrix renders the resulting nanocomposites applicable in devices such as photovoltaic (solar) cells [11], polymer-electrolyte membrane fuel cells [12], and magnetic data storage systems. The functional groups of the polymer surrounding the nanoparticles enable these nanocomposites to be used for various industrial applications, such as site-specific molecule targeting applications in the biomedical areas and explosive detection sensors [13]. High particle loading, required for certain applications such as solar cells, electromagnetic interfaces (EMI), microwave absorbers [14–16] and giant magnetoresistance (GMR) sensors [17], usually has a deleterious effect on the mechanical properties due to the particle agglomeration and poor interfacial bonding between the nanoparticle and polymer matrix. Therefore, particles are functionalized by a surfactant or a coupling agent to achieve uniform particle dispersion in the matrix and chemical bonding at the interface.

Vinyl ester resin has been widely used in the marine (Naval submarine) industry [18] due to its good mechanical properties such as large Young's Modulus and tensile strength, and its superior resistance to moisture and chemicals [19]. As a thermosetting material, vinyl ester resin can be cured easily in an ambient condition and was reported to strongly depend on curing temperature, initiators and accelerator levels [20]. Our recent investigations on nanocomposites reinforced with different ceramic nanoparticles, such as alumina, zinc oxide, iron oxide and copper oxide, have shown that the ceramic nanoparticle itself has some effect on the curing process and subsequent performance of nanocomposites [19,21,22]. However, there still lacks a systematic study of the nanoparticle effect on the curing process for high-quality vinyl ester resin nanocomposite fabrication, especially for the case of reactive magnetic metallic

* Corresponding author. Tel.: +1 310 206 8157.
E-mail addresses: nanomaterials2000@gmail.com, zguo@my.lamar.edu (Z. Guo).
[1] Assistant Professor in Chemical Engineering Department, Lamar University, Beaumont, Texas, 77710, USA.

0266-3538/$ - see front matter © 2008 Elsevier Ltd. All rights reserved.
doi:10.1016/j.compscitech.2008.05.017

nanoparticles. In addition, the functionalization of nanoparticles made the composite fabrication more complicated and costly.

In this paper, we present a facile and economical method to prepare iron nanoparticles reinforced vinyl ester resin nanocomposites. There is no need of any additional surfactant or coupling agent for improving the particle dispersion and enhancing the particle/matrix interaction. The monomers, serving as a stabilizer, are covalently bound onto the nanoparticle surface and further copolymerize with the extra monomers after the introduction of the catalyst and promoter. The mechanical and magnetic properties of the nanocomposites were explored. The stabilization mechanism of the nanoparticles by monomers for nanocomposite fabrication was investigated by X-ray photoelectron spectroscopy (XPS).

2. Experimental

2.1. Materials

The polymeric matrix used was a vinyl ester resin, Derakane momentum 411–350 (manufactured by the Dow Chemical Company), which is a mixture of 55 wt% vinyl ester with an average molecule weight of 970 g/mole and 45 wt% styrene monomers. Styrene with only one unsaturated carbon–carbon double bond provides linear chain extension. Vinyl ester monomers with two reactive vinyl end groups enable the cross-linking for network formation. The liquid resin has a density of 1.045 g/cm^3 and a viscosity of 350 centipoises (cps) at room temperature. Trigonox 239-A (curing catalyst or initiator, organic peroxide, liquid) was purchased from Akzo Nobel Chemicals. Cobalt naphthenate (CoNap, OM Group, Inc.) was used as a catalyst promoter (accelerator) to decompose the catalyst at room temperature. Iron (QuantumSphere, Inc., Santa Ana, CA) nanoparticles with an average diameter of 20 nm and a specific surface area of 35–55 m^2/g (BET) were produced and transported in the inert gas to prevent the oxidation. The active nanoparticles were used as nanofillers for the nanocomposite fabrication and also served as a metal precursor for the displacement between the monomers and the metals.

2.2. Nanocomposite fabrication

The nanocomposite fabrication is briefly described as follows. A specific amount of iron nanoparticles with an average size of 20 nm (provided by QuantumSphere Inc.) and the nitrogen degassed vinyl ester resin (30 g) are transferred into a 2-neck flask. The sealed flask is ultrasonically stirred for about 2 h to completely wet the nanoparticles by the resin. The suspended solution is further stirred by hand and ultrasonically for another 2 h until uniform dispersion is obtained. A mixture of the nitrogen-degassed catalyst (2.0 wt%, Trigonox 239-A, organic peroxide, Akzo Nobel Chemicals) and promoter (0.3 wt%, cobalt naphthenate, OM Group, Inc.) is introduced quickly. The final solution is poured into a silicone mold for room temperature curing. All the reactants are added in an ultrahigh purity nitrogen protection condition. Caution: Handling of the iron nanoparticles should be done in a fume hood, due to high risk of fire and respiratory health issue.

2.3. Characterization

The optimum curing condition was investigated by a differential scanning calorimetry (DSC) with a heating rate of 20 °C/min and a nitrogen flow rate of 10 cm^3/min (ccpm). The reaction enthalpy (J/g) and residual heat of reaction were measured from the area under the DSC peaks.

Nanocomposites with different particle loadings were fabricated based on the functionality of the vinyl ester resin monomers and the reactivity of the metal nanoparticles. Weight percentage of nanoparticles in the nanocomposites and thermal stability of the nanocomposites were determined by the thermo-gravimetric analysis (TGA, PerkinElmer) with an argon flow rate of 50 ccpm and a heating rate of 10 °C/min.

The dispersion quality of the nanoparticles in the vinyl-ester resin matrix was investigated by scanning electron microscopy (SEM) on the polished nanocomposite cross-sectional area. The SEM samples were carefully prepared as follows. The cured composite samples were polished with a 4000-grit sand paper and a following 50 nm alumina nanoparticle aqueous solution polishing to achieve a smooth surface, then washed with DI water, and followed by sputter coating a 3 nm gold. The fracture surface of the nanocomposites after the tensile test was sputter coated with a 3 nm gold studied for SEM investigation.

X-ray photoelectron spectroscopy (XPS) was utilized to investigate the nanocomposite formation mechanisms. XPS was conducted on a Kratos Axis Ultra XPS system using a monochromatic Al Kα source for irradiation. The sample was prepared by allowing complete reaction between the nanoparticles and vinyl ester resin monomers under ultrasonication without curing, then washing with excessive anhydrous tetrahydrofuran to remove excessive resin.

The mechanical properties were evaluated by tensile tests following the American Society for Testing and Materials standard (ASTM, 2005, standard D 1708-02a). An Instron 4411 with Series IX software testing machine was used to measure the tensile strength and Young's modulus. The dog-bone shaped specimens were prepared as described in the nanocomposite fabrication section. The specimen surfaces were smoothed with an abrasive sand paper (1000 grit). A crosshead speed of 15 mm/min was used and strain (mm/mm) was calculated by dividing the crosshead displacement (mm) by the gage length (mm).

The magnetic properties were investigated in a 9-T Physical Properties Measurement System (PPMS) by Quantum Design.

3. Results and discussion

The iron nanoparticles were observed to have a significant effect on the curing process as investigated by DSC. The initial and peak exothermal curing temperatures were substantially decreased after the incorporation of nanoparticles in the liquid resin. The released reaction heat (based on the neat resin) decreased with the increase of the particle loading as marked in Fig. 1. The lower initial exothermal curing temperature indicates that the addition of iron nanoparticles favors a lower temperature curing.

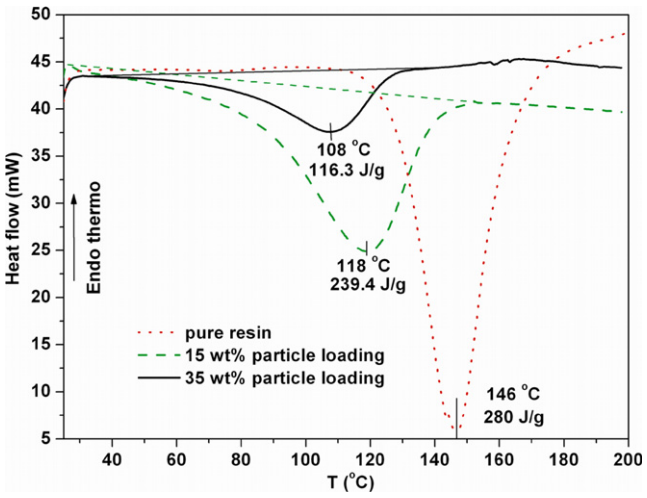

Fig. 1. DSC curves of the liquid pure resin and vinyl ester nanocomposites with different iron nanoparticle loadings.

The DSC study on the 24-h room temperature cured nanocomposites showed a similar 75% polymerization for composites with two different loadings. However, a lower curing temperature is observed in composites with a higher particle loading, shown in Fig. 2. As compared to the lower initial curing temperature in the liquid composite samples, the higher initial curing temperature in the composites after 24-h room-temperature curing is due to larger molecule chains which require more energy for further polymerization. In contrast to the lower reaction heat in the liquid nanocomposites with higher particle loading, the room temperature cured nanocomposites with higher particle loading have higher reaction heat. This is due to more monomers surrounding the particle surface with a less molecular mobility for polymerization.

Fig. 3 shows the thermo-gravimetric analysis (TGA) curves of the room-temperature cured vinyl ester resin nanocompsoites reinforced with different particle loadings. Vinyl ester resin in the 24-h room-temperature cured nanocomposites is observed to be stable at temperatures lower than 300 °C and decompose at temperatures higher than 300 °C. The slight weight loss in the range of 100–300 °C in the composites with low particle loadings is due to the monomer evaporation.

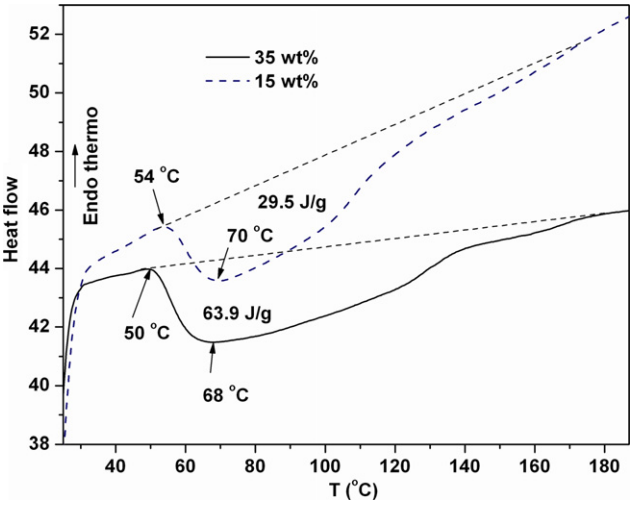

Fig. 2. DSC curves of the vinyl ester nanocomposites after a 24-h room-temperature curing.

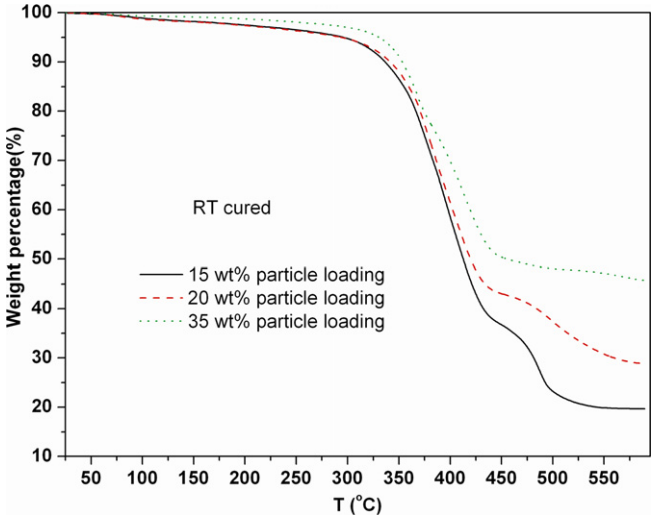

Fig. 3. TGA curves of the nanocomposites with different particle loadings after 24-h room temperature curing.

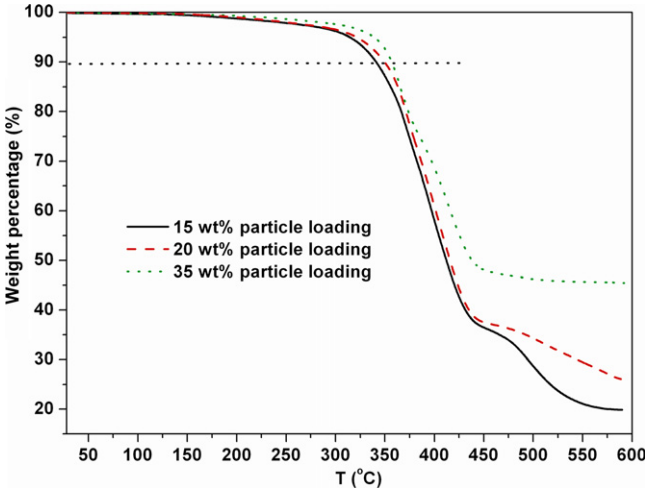

Fig. 4. TGA curves of the nanocomposites with different particle loadings after postcuring at 100 °C.

A fully cured nanocomposite with a 100% curing extent was deduced after postcure at 100 °C for 2 h with an observed straight line in the DSC curves (not shown here). The thermal stability of the fully cured nanocomposite was investigated by thermo-gravimetric analysis (TGA). Fig. 4 shows the TGA curves of the fully-cured nanocompsoites with different particle loadings. The fabricated polymer nanocomposites can resist to higher temperatures above 300 °C or even higher with the increase of the particle loading. Iron nanoparticles were reported to serve as a catalyst for carbon nanotube/nanofiber formation and may decrease the thermal stability of the nanocomposites. However, the enhanced thermal stability is due to the following synergistic effects. The nanoparticles lower the mobility of the polymer chains which were chemically bounded onto the nanoparticle surface. The bounded polymer, on the other hand, inhibits the active component of elemental iron to catalyze the polymer by forming an iron-vinyl ester complex. The mechanism of the reaction was investigated by X-ray photoelectron spectroscopy (XPS) and will be discussed later.

The tensile mechanical properties of the fully cured nanocomposites are summarized in Table 1. The Young's Modulus and tensile strength increased 170% and 20%, respectively in the 35 wt% nanocomposite. However, the tensile strength decreased in the 50 wt% nanocomposite because of the noticeable voids.

The particle distribution within the cured vinyl ester resin matrix was characterized by a field emission scanning electron microscope (SEM). Fig. 5a shows the typical SEM micrograph of the cross-sectional area of the nanocomposite with a particle loading of 35 wt%. The particles show different sizes in the SEM micrographs. This is due to the particles embedding in different depth in the vinyl ester resin matrix. However, no particle pull-out (i.e., voids) in the samples after polishing was observed indicating a

Table 1
Mechanic properties of the cured pure resin and nanocomposites

Particle loading (wt%)	Young's Modulus (GPa)	Tensile strength (MPa)
0	1.2 0 ± 0.10	55.20 ± 2.60
15	2.35 ± 0.45	55.37 ± 0.70
35	3.24 ± 0.78	63.09 ± 1.20

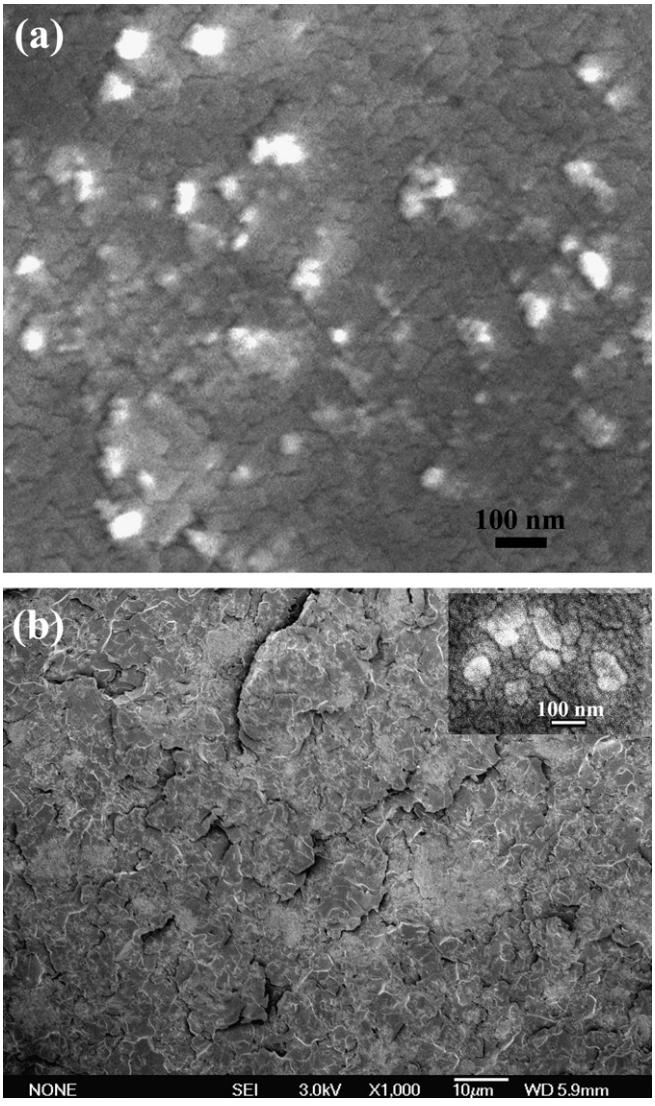

Fig. 5. SEM micrograph of (a) the cross-section and (b) fracture surface after tensile test of the nanocomposites with a particle loading of 35 wt%.

strong chemical bondage between the nanoparticles and the vinyl ester resin matrix.

Fig. 5b shows the SEM micrographs of the fracture surface after the tensile test. A rougher fracture surface with many openings was observed in the nanocomposites as compared to the fracture surface characterized by larger smooth areas, ribbons and fracture steps observed in the cured pure vinyl ester resin [19]. This micro-rough structure is attributed to the matrix shear yielding or local polymer deformation between the nanoparticles rather than the intra-particle propagating cracks due to the difficulty in breaking the harder iron nanoparticles. No void/holes arising from the possible peeling off the nanoparticles from the polymer matrix were observed in the high-resolution SEM micrograph as shown in the inset of Fig. 5b, which is similar to the polished cross-sectional composite sample and indicates a strong chemical interaction between the nanoparticles and vinyl ester resin matrix. The strong interfacial interactions between the nanoparticles and the vinyl ester resin matrix thus have an important effect on the effective transfer of the local stress. The extremely higher specific surface area inherent with the nanoscale particles as compared to the bulk/micron particles together with the strong interfacial chemical bondage between the polymer matrix and the reinforcing nanoparticles effectively facilitate the local stress transfer from the polymer matrix to the tougher metal nanoparticles, which results in a much higher tensile strength as compared with the cured pure vinyl ester resin.

Fig. 6 shows the room-temperature magnetic hysteresis loop of the as-prepared vinyl ester monomer stabilized iron nanoparticles and the iron nanoparticles reinforced vinyl ester resin nanocomposites with different particle loading. The monomer stabilized iron nanoparticles were prepared by displacement reaction between iron nanoparticles and vinyl ester resin in ultrasonication and nitrogen protection conditions, washing with tetrahydrofuran and drying in a vacuum oven. As compared to the reported coercive force (coercivity, H_c, the magnitude of the external applied magnetic field necessary to return the magnetic material to a zero magnetization condition.) of 5 Oe for the bare superparamagnetic iron nanoparticles [17], H_c is observed to increase to 153 Oe after nanoparticles stabilized with vinyl ester monomers and further increased to 226.5 Oe in the vinyl ester resin nanocomposite with a particle loading of 35%. This observation indicates that the bare superparamagnetic iron nanoparticles became harder (ferromagnetic state at room temperature) after they were dispersed in a polyurethane matrix and consistent with the nanoparticles dispersed in the polyurethane matirx [17]. The big discrepancy in the coercivity is due to the decreased interparticle dipolar interaction arising from the increased interparticle distance of nonmagnetic oreganics [23] as compared to the close contact of the pure iron nanoparticles, and also due to the polymer-particle interfacial effect [24]. The organic spacers are either the monomers chemically bound onto the nanoparticle surface in the monomer stabilized iron nanoparticles or the physical presence of vinyl ester resin matrix around iron nanoparticles with monomers chemically bound onto the nanoparticle surface in the fully cured vinyl ester resin nanocomposites.

The magnetization of the monomer stabilized iron nanoparticles and the fully cured vinyl ester resin nanocomposite does not saturate at higher field as shown in Fig. 6. Saturation magnetization (M_s) was determined by the extrapolated saturation magnetization obtained from the intercept of the magnetization *vs* H^{-1} at high field [24,25]. The calculated M_s was 30.5 emu/g, 52.5 emu/g and 73.0 emu/g for the vinyl ester resin nanocomposites with a particle loading of 15 wt% and 25 wt% and 35 wt%, respectively.

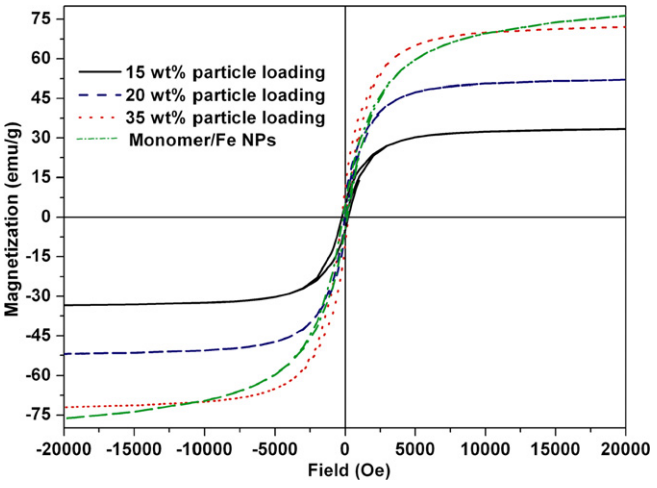

Fig. 6. Room temperature magnetic hysteresis loops of vinyl ester resin monomer stabilized iron nanoparticles and the iron nanoparticles reinforced vinyl ester resin nanocomposites with different particle loading.

M_s based on the pure iron nanoparticles was about 203 emu/g, 210 emu/g and 209 emu/g for nanocomposites with a particle loading of 15 wt%, 25 wt% and 35 wt%, respectively. All these values are a little lower than that of the bulk iron (218 emu/g),[26] which is due to the loss of the active magnetic iron on the nanoparticle surface arising from the iron oxidation either by the displacement or exposure to air during the composite fabrication.

The iron nanoparticle is reported[27] to have a superparamagnetic zero-coercivity region of 10 nm and a critical size of 100 nm with a maximum coercivity. The coercivity decreases to that of the bulk iron when the nanoparticles become agglomerate with size of microscale. The observed larger coercivity in the nanoparticles after dispersed in the polymer matrix further indicates a fairly uniform dispersion of nanoparticles in the polymer matrix, i.e., the nanoparticles are stabilized by the vinyl ester monomers without agglomeration. Gas bubbles were observed during the particle dispersion in the vinyl ester resin in the air-free nitrogen condition. This is due to the hydrogen generation arising from the displacement reaction between reactive metallic iron nanoparticles and vinyl ester monomers. The nature of the interaction between the nanoparticles and the vinyl ester monomers was investigated by XPS investigation and the XPS samples were prepared carefully as described in Experimental section. Fig. 7 shows the high resolution carbon 1 s XPS spectra with all the fitting curves representing different functional groups. The peaks at 284.6 eV, 285.0 eV, 286.6 eV and 288.6 eV represent C–C and/or C–H, C=C and/or C–H, C–O and C=O bonds, respectively. These characteristic peaks arise from the vinyl ester resin and thus indicates the presence of vinyl ester resin on the nanoparticle surface. Iron 2p3/2 high resolution XPS spectrum verified partial oxidation

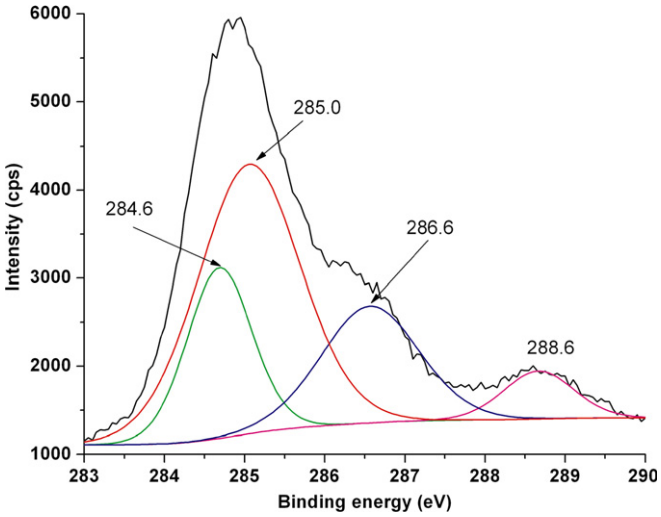

Fig. 7. High-resolution carbon 1s XPS spectrum of THF washed vinyl ester/iron nanoparticle complex.

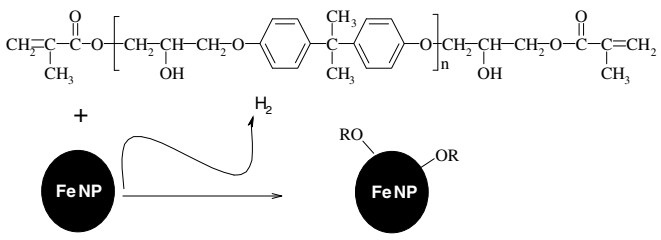

Scheme 1. Vinyl ester stabilization of iron nanoparticles, OR represents the hydroxyl group in vinyl ester.

of the iron nanoparticle surface arising from the displacement of the vinyl ester resin on the nanoparticle surface.

The nanocomposite formation mechanisms are shown in Scheme 1. The active metallic iron nanoparticles react with the hydroxyl functional groups of the vinyl ester monomers and release hydrogen. The vinyl ester monomer serves as a surfactant with one side chemically bound onto the nanoparticle surface. The other side promotes the dispersion of the nanoparticles in the monomer solution. The subsequent addition of the catalyst and promoter serves as a free radical to initiate the monomer polymerization for crosslinkage formation. The carbon–carbon double bonds of the vinyl ester monomers bound onto the nanoparticles also copolymerize with the unbound monomers (styrene for polymer chain growth or vinyl ester monomers for polymer cross-linking growth) to form a robust nanocomposite. The strong chemical bondage between the nanoparticles and the vinyl ester matrix enhances the mechanical properties. The linked vinyl ester serves as a spacer to separate the nanoparticles leading to an observed larger coercivity [23]. The crosslinked vinyl ester resin matrix provides the protection for the iron nanoparticles from further oxidation and dissolution in acidic environments [19].

4. Conclusions

In conclusion, we have demonstrated a simple approach to fabricate a robust vinyl ester resin nanocomposite reinforced with iron nanoparticles. Without any additional surfactant or coupling agent, the resin is chemically bound onto the nanoparticle surface and protects the iron nanoparticles from agglomeration and oxidation. Tensile strength and Young's Module are larger than those of cured pure resin. The resulting magnetically harder nanocomposites with an increased thermal stability are ferromagnetic at room temperature and have potential applications in the marine systems, magnetoresistive sensors [17] and microwave absorption systems[15].

Acknowledgements

This work was supported by QuantumSphere Research Grant (QuantumSphere Inc.), UC-discovery Grant ELE06-10268, and the Air Force Office of Scientific Research through AFOSR Grant FA9550-05-1-0138. DPY kindly acknowledges support from the National Science Foundation under Grant No. DMR 04-49022.

References

[1] Lu A-H, Salabas EL, Schueth F. Angew Chem Int Ed 2007;46:1222.
[2] Guo Z, Kumar CSSR, Henry LL, Doomes EE, Hormes J, Podlaha EJ. J Electrochem Soc 2005;152:D1.
[3] Cho S-J, Kauzlarich SM, Olamit J, Liu K, Grandjean F, Rebbouh L, et al. J Appl Phys 2004;95:6804.
[4] Guo Z, Henry LL, Palshin V, Podlaha EJ. J Mater Chem 2006;16:1772.
[5] Guo Z, Moldovan M, Young DP, Henry LL, Podlaha EJ. Electrochem Solid State Lett 2007;10:E31.
[6] Castro C, Ramos J, Millan A, Gonzalez-Calbet J, Palacio F. Chem Mater 2000;12:3681.
[7] Yong V, Hahn HT. Nanotechnology 2004;15:1338.
[8] Mack JJ, Viculis LM, Ali A, Luoh R, Yang G, Hahn HT , et al. Adv Mater 2005;17:77.
[9] Sandi G, Joachin H, Kizilel R, Seifert S, Carrado KA. Chem Mater 2003;15:838.
[10] Sanchez C, Julian B, Belleville P, Popall M. J Mater Chem 2005;15:3559.
[11] Beek WJE, Wienk MM, Jassen RAJ. Adv Mater 2004;16:1009.
[12] Navarra MA, Croce F, Scrosati B. J Mater Chem 2007;17:3210.
[13] Toal SJ, Trogler WC. J Mater Chem 2006;16:2871.
[14] Praveen S, Babbar VK, Archana R, Puri RK, Goel TC. J Appl Phys 2000;87:4362.
[15] Guo Z, Park S, Hahn HT, Wei S, Moldovan M, Karki AB, et al. J Appl Phys 2007;101:09M511.
[16] Brosseau C, Queffelec P, Talbot P. J Appl Phys 2001;89:4532.
[17] Guo Z, Park S, Hahn HT, Wei S, Moldovan M, Karki AB, et al. Appl Phys Lett 2007;90:053111.
[18] Sorathia U, Rollhauser CM, Hughes WA. Fire Mater 1992;16:119.
[19] Guo Z, Pereira T, Choi O, Wang Y, Hahn HT. J Mater Chem 2006;16:2800.

[20] Abadie MJM, Mekhissi K, Burchill PJ. J Appl Poly Sci 2002;84:1146.
[21] Guo Z, Wei S, Shedd B, Scaffaro R, Pereira T, Hahn HT. J Mater Chem 2007;17:806.
[22] Guo Z, Liang X, Pereira T, Scaffaro R, Hahn HT. Compos Sci Technol 2007;67:2036.
[23] Kechrakos D, Trohidou KN. Phys Rev B 1998;58:12169.
[24] Cullity BD. Introduction to magnetic materials. New York: Addison-Wiley; 1972.
[25] Skumryev V, Stoyanov S, Zhang Y, Hadjipanayis G, Givord D, Nogues J. Nature 2003;423:850.
[26] Brosseau C, Talbot P. J Appl Phys 2005;97:104325-1/11.
[27] Huber DL. SMALL 2005;1:482–501.